Sustainable strategies to synthesize small-pore NaP zeolites using natural minerals

José Adán Moreno Torres[a], *Fabricio Espejel-Ayala*[b], *Rafael Ramírez-Bon*[a, *], *Eduardo Coutino-Gonzalez*[c, *]

[a]Centro de Investigación y de Estudios Avanzados del IPN, Unidad Querétaro, Apdo. Postal 1-798, 76001, Querétaro, Querétaro, México.

[b]Centro de Investigación y Desarrollo Tecnológico en Electroquímica. Parque Tecnológico Querétaro, s/n. Pedro Escobedo, Querétaro, México

[c]Sustainable Materials Unit, VITO Flemish Institute for Technological Research, B-2400, Belgium.

AUTHOR INFORMATION

Corresponding Authors

*rrbon@cinvestav.mx, ecoutino@vito.be

ABSTRACT

The interesting chemical and physical properties of microporous zeolites have led to their use in numerous industrial applications, such as adsorbents, ion exchangers, and catalysts, increasing the worldwide consumption of these materials annually. However, the development of synthetic zeolites usually involves the use of expensive chemical reagents; therefore, the use of alternative sources of Si and/or Al, such as minerals and waste streams, has gained attention over the past few years owing to the benefits in production costs and decreasing environmental burden. In this study, we report the synthesis of single-phase small-pore NaP zeolites via alkaline hydrothermal treatment (HT) using natural clinoptilolite (CLIP) as the Si and Al source. The synthesized zeolites were analyzed using X-ray diffraction, electron microscopy, energy dispersive spectroscopy, and X-ray photoelectron spectroscopy. The results showed that the variations in molar concentration (1 and 2 M), crystallization time (24 and 39 h), and crystallization temperature (90, 105, and 110 °C) play a major role in obtaining two types of NaP isomorphs (NaP1 and NaP2), which feature a flexible framework, where the synthesis parameters of 1 M, 24 h, and 90 °C led to the

formation of a single-phase NaP1 zeolite with high purity. These results demonstrate the feasibility of developing sustainable synthesis processes from low-cost and abundant raw materials to produce high-value-added synthetic zeolites as alternatives to traditional chemical reagent-based synthesis methods.

***Keywords**:* NaP1-NaP2 zeolites; natural clinoptilolite; sustainable protocols; valorization.

TOC Graphic:

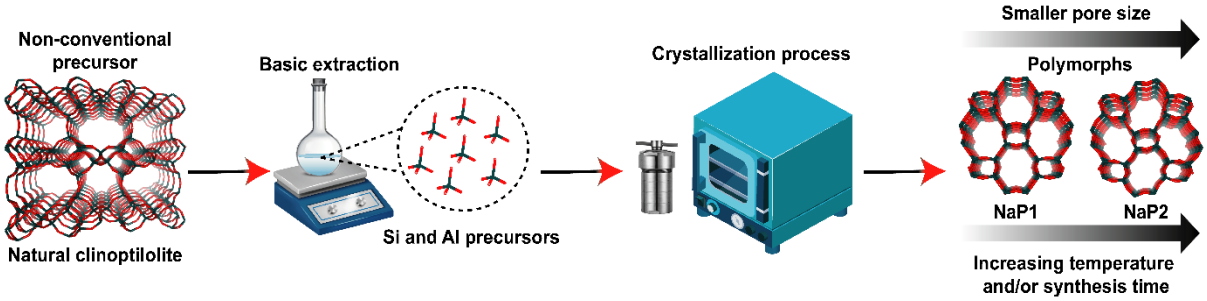

1. Introduction

Zeolites are a family of open-framework aluminosilicate materials with structures based on a three-dimensional network of AlO_4 and SiO_4 tetrahedra linked by oxygen bridges [1]. These materials have channels and voids that allow intracrystalline transport, adsorption, and diffusion of ions and molecules [2]. Owing to these unique characteristics, zeolites have several applications such as highly efficient catalysts, detergents, adsorbents, and ion exchangers. Among the different types of existing zeolite topologies, NaP zeolites belonging to the zeolites P group and classified as synthetic analogs of natural gismondine-type (GIS) zeolites, possess a micropore size (~2.90 Å) smaller than those of other zeolite structures such as LTA (~4.10 Å), MFI (~5.40 Å), MOR (~6.70 Å), LTL (~7.10 Å), and FAU (~7.40 Å), highlighting their molecular sieve properties [3]. Structurally, zeolite P is composed of secondary building units (SBU) containing four- and eight-membered rings (4-MRs and 8-MRs) of T atoms (T = Si or Al linked together by sharing oxygen atoms) and possesses a three-dimensional (3D) pore system with two intersecting 8-MRs of different dimensions [4]. Zeolites with a GIS-like framework have been described as the most open [tetrahedral] framework type generated thus far because of the high flexibility of the Si–Al linkage in their topology, which induces different real symmetries depending on the extra-framework cations, Si/Al ratio, and degree of dehydration [5]. Owing to their unusual flexibility, different

crystalline polymorphs possessing a GIS framework type have been reported in the literature, such as cubic (also referred as P1, P_c, or cubic P) and tetragonal (also referred as P2, P_t, or tetragonal P) [6–8]. For instance, Oleksiak *et al.* [7] reported the synthesis of P1 and P2 zeolites using a hydrothermal method at 100 °C for 1 to 7 days using a colloidal silica source.

Synthetic zeolites exhibiting high crystalline purity and uniform size, along with improved ion exchange capabilities, are often produced from commercial aluminates (e.g., aluminum (hydr)oxides, nitrates, alkoxides, etc.) and silicates (e.g., colloidal silica, alkali silicates, silicon alkoxides such as tetraethyl orthosilicate) by hydrothermal processes in an alkaline medium [9–11]. Nonetheless, the preparation of synthetic zeolites from these starting materials is relatively expensive, and close contact with certain alkoxysilane compounds can be harmful to health [12]. Therefore, it is necessary to develop environmentally friendly, inexpensive, and nontoxic precursors. Alternative sources of silica and alumina are natural minerals and solid waste, such as fly ash, metakaolin, diatomite, and smectite, as low-cost raw materials to produce high-purity synthetic zeolites [13]. Among natural minerals, clinoptilolite (CLIP) with a Heulandite (HEU)-type framework is considered one of the most abundant natural zeolites on Earth, with low extraction costs that can be used as Si and Al sources for producing industrially appealing zeolites [14, 15]. For instance, the preparation of synthetic zeolites, such as NaP, from natural CLIP zeolites using conventional and ultrasound-assisted hydrothermal methods has been reported [13–21].

Several studies have reported different strategies for the synthesis of NaP from CLIP. For example, Kang *et al.* [18] and Wang *et al.* [13] obtained NaP zeolite with and without the sodium hydroxide fusion method prior to hydrothermal reaction using natural CLIP zeolite. In other studies employing the alkaline hydrothermal route, pure chemical reagents such as NaCl [16], $Al(OH)_3$ [19], and $NaAlO_2$ [20] were added during the CLIP reaction in an alkaline medium, increasing the production costs of NaP zeolite. In contrast, novel techniques have been used to reduce the crystallization time and increase the purity of the synthesized zeolite. Behin et al. employed an ultrasound-assisted hydrothermal process to convert CLIP into NaP. After 5 h of sonication in an alkaline medium, a complete NaP phase formation was obtained [14]. However, such techniques require sophisticated instrumentation, and the production of such materials is often limited. And recently, Hong S *et al*. [21] proposed the transformation of CLIP to NaP by a "top-down approach" hydrothermal reaction, where CLIP was used in granular size, using 3 M NaOH solution in a 96 °C oven and obtaining a

NaP phase after 60 h of crystallization. Therefore, further research is needed on NaP zeolite synthesis, with a focus on protocols to make their manufacturing more sustainable and cost-competitive.

In the present work, we report the preparation of small-pore NaP1 and NaP2 zeolites obtained from CLIP as non-conventional precursor by alkaline hydrothermal treatment (HT). First, CLIP was subjected to pretreatment in an alkaline dissolution to extract Si and Al precursors; subsequently, this dissolution was subjected to a crystallization process, where the effects of alkalinity, temperature, and crystallization time were studied. The results showed that high-purity NaP1 zeolite could be obtained at 1 M NaOH concentration, 90 °C, and 24 h HT, whereas increasing the hydrothermal conditions to 2 M NaOH for 110 °C at 39 h led to the production of the NaP2 zeolite phase. Furthermore, this method demonstrates the feasibility of developing high-purity synthetic zeolites, reducing costs, and decreasing the use of commercial reagents. Our findings open the possibility of extending the use of natural CLIP as a starting material for the development of different types of zeolites through synthetic routes, such as dry solid fused alkali reagents.

2. Materials and methods

2.1 Starting material and reagents

Natural CLIP [$(Na, K)_6Si_{30}Al_6O_{72}\cdot nH_2O$] was used as non-conventional Si- and Al- source for the zeolite synthesis, which is abundant in the central-southern region of Mexico with HEU topology and a framework density of 17.5 T-atoms/1000 $Å^3$. The CLIP precursor was manually crushed into a fine powder and calcined at 450 °C for 5 h to remove organic impurities prior to its use. Anhydrous NaOH pellets (purity ≥ 98 %, Sigma-Aldrich) were used as received.

2.2 Synthesis of NaP zeolites

Grinded CLIP was added to different NaOH molar aqueous solutions (1 M and 2 M in deionized water) in PTFE bottles using a CLIP (g): NaOH (g) ratio of 0.75 (more details are provided in the supporting information). The suspension was heated at 90 °C for 6 h under vigorous stirring, filtered through a Büchner funnel, and the supernatant was poured into a

Teflon vessel inside a stainless-steel autoclave that was placed in an oven at different crystallization temperatures (90, 105, and 110 °C) and times (24 and 39 h). After HT, the autoclave was quenched in cold water, and the precipitate was recovered by centrifugation, washed three times with 50 ml of deionized water, dried at 80 °C for 3 h, weighed, transferred to vials, and stored in a desiccator for further characterization. The procedure is illustrated in Figure 1.

2.3 Material characterization

Scanning electron microscopy (SEM) and energy dispersive spectroscopy (EDS) analyses were conducted using a JEOL 6500LV device equipped with an X Flash 6110 Bruker detector. Particle size distributions were estimated from SEM images using ImageJ processing software (30–50 zeolite crystals on average). X-ray diffraction (XRD) analysis was performed on a D8 Advance Bruker in the range of $2\theta = 5 – 50°$ at a scanning speed of 0.02 °/s. The XRD patterns were indexed according to the standard CLIP and NaP1 zeolite diffraction patterns listed in the International Zeolite Association (IZA) [22], and the X'Pert High Score Plus software was used to simulate the NaP2 zeolite diffraction pattern. X-ray photoelectron spectroscopy (XPS) was performed using a Thermo Scientific K-Alpha XPS System. The AlKα source produces X-rays radiation of 1486.7 eV that is focused to a 200 x 200 μm^2 spot (power density = 66 W/m^2). Fourier transform infrared spectroscopy (FTIR) spectra of the samples were recorded in air at room temperature using attenuated total reflectance Fourier transform infrared spectroscopy (ATR-FTIR). The spectra were recorded using a Thermo Scientific Nicolet 6700 spectrometer in the wavenumber range 4000–550 cm^{-1} with 32 scans. Thermogravimetric analysis (TGA) analysis was performed on a Q500 TGA device from TA Instruments. Between 10 and 30 mg of the zeolite sample was introduced in a platinum sample holder. During the analysis, the sample was heated with a rate of 3 °C per minute to 600 °C under a constant air flow.

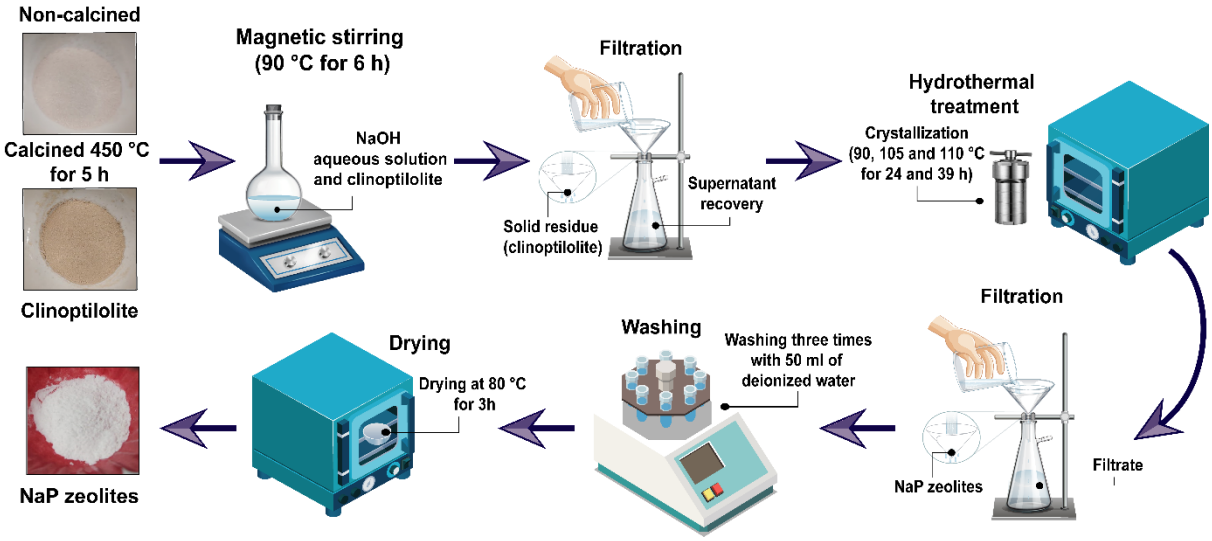

Figure 1. Experimental procedure for basic extraction/hydrothermal treatment used to synthesize NaP zeolites from CLIP.

3. Results and discussion

3.1 Characterization of natural CLIP precursor

Figure 2a shows the XRD pattern of the raw CLIP used as the starting material. The presence of CLIP was confirmed to be the only crystalline phase according to the JCPDS (01-079-1461) reference file [22]. The surface morphology of the CLIP zeolite was analyzed by SEM, displaying crystals with irregular morphology and a rough surface, as observed in Figure 2b. Elemental analysis conducted by EDS (Figure 2c) reveals a Si/Al ratio of 4.8, thereby proving a CLIP zeolite phase, since HEU and CLIP, despite having the same structural topology, differ in having a different Si/Al ratio (Si/Al<4 for HEU and Si/Al > 4 for CLIP) [23]. The EDS spectrum (Figure S1) indicates that CLIP is mainly composed of Si, O, and Al, as they form the framework of the zeolite structure, and the elemental mapping (Figure 2c) exhibits a homogeneous distribution of the elements. These results also reveal the presence of several extra-framework cations, such as K^+, Ca^{2+}, Mg^{2+}, Na^+, and Fe^{2+}, with K + being the most prevalent exchange cation and Fe^{2+} as the cation with the lowest atomic concentration. The presence of these extra-framework cations and organic impurities directly affects the coloration of the precursor, showing light and strong beige coloration before and after calcination, respectively (Figure 1). Importantly, the CLIP used in this study was calcined at 450 °C for 5 h before use. Since it has been described that calcination of raw materials (such as clay minerals) at high temperatures (500-800 °C) can also be used as

another thermal pre-treatment to increase the solubility of Si and Al species in zeolite production [24].

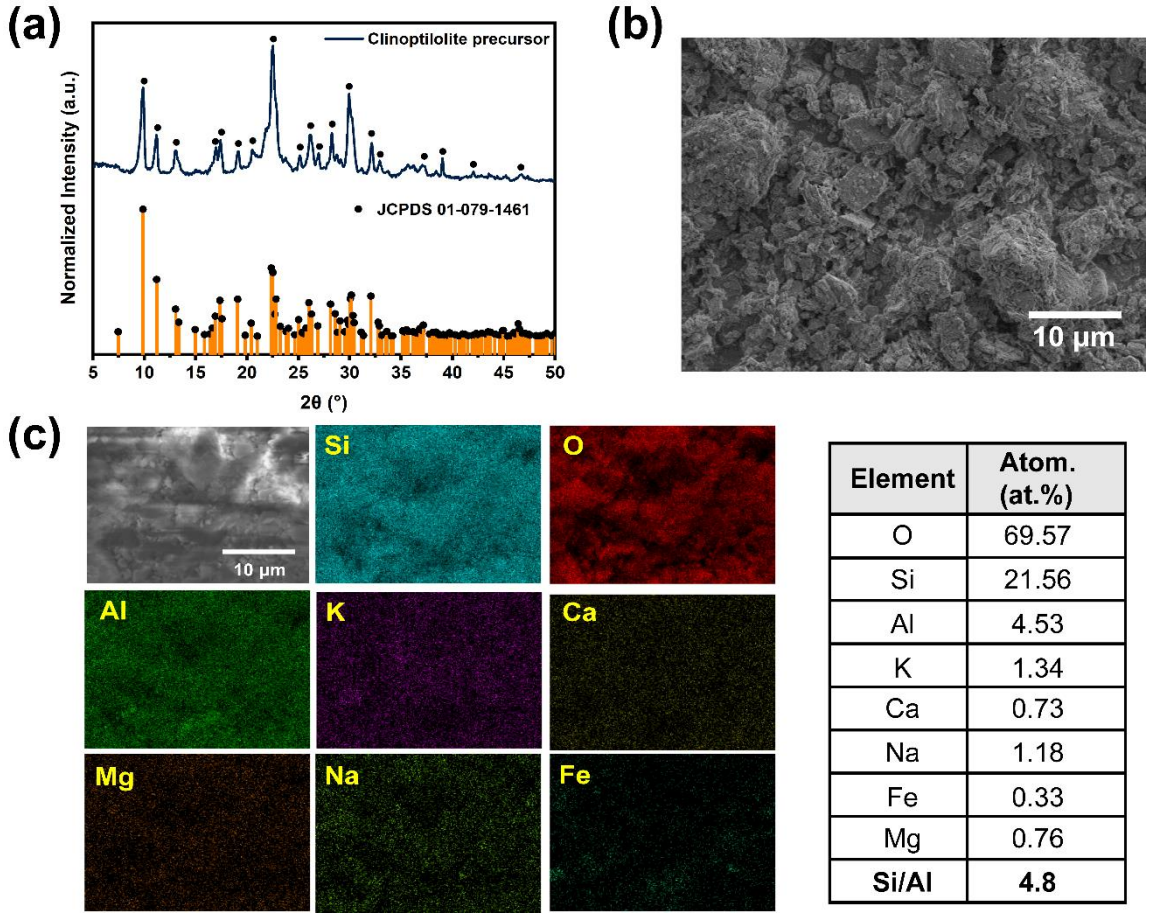

Element	Atom. (at.%)
O	69.57
Si	21.56
Al	4.53
K	1.34
Ca	0.73
Na	1.18
Fe	0.33
Mg	0.76
Si/Al	**4.8**

Figure 2. (a) XRD pattern, (b) SEM micrograph, and (c) elemental mapping and atomic concentration of elements of the natural CLIP precursor employed as starting material for zeolite synthesis.

3.2 Effect of alkalinity in as-synthesized NaP1 zeolites using CLIP

The effect of varying the NaOH concentration (1 and 2 M) on the synthesis of NaP-type zeolites starting from natural CLIP through alkaline dissolution and HT was investigated. The first synthesis batch, performed with 1 M NaOH for 24 h at 90 °C, yielded P-type zeolite. Figure 3a shows the diffractogram of the as-synthesized NaP zeolite, which shows the characteristic peaks of NaP1-type zeolite compared to the IZA NaP1 zeolite pattern (JCPDS No. 71-0962) [8, 22, 25], without the presence of amorphous or other crystalline impurities, suggesting the formation of single-phase NaP1 zeolite after the hydrothermal process. SEM analysis (Figure 3b) reveals that the as-synthesized NaP1 exhibits cuboctahedron-shaped

crystals, similar to those described in previous reports [26–28]. In addition, Figure 3c displays the histogram of the particle size distribution, which ranges between 2.6 and 6.6 µm centered at 4.3 µm.

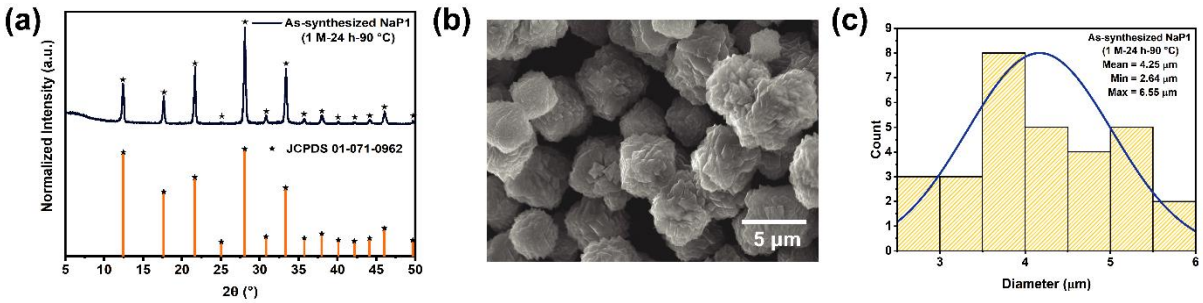

Figure 3. (a) XRD pattern, (b) SEM micrograph, and (c) particle size distribution analyzed using ImageJ (calculated from 30 to 50 particles) of NaP1 zeolites synthesized with 1 M NaOH for 24 h at 90 °C.

Figure S2 shows the FTIR spectra comparison between the natural CLIP precursor and the zeolite obtained with 1 M, 24 h and 90 °C, providing additional information to validate the zeolite synthesis. The presence of adsorbed water is evidenced in the spectra through the water bending vibration at 1618 cm^{-1} (Figure S2a) [29]. The bands observed at 967 and 674 cm^{-1} correspond to internal vibrations of the Si-O-Si and Si-O-Al bridges in the zeolite. Likewise, the bands at 739 and 598 cm^{-1} are attributed to symmetric bonds and Si and Al-O bonds, respectively [30]. Nevertheless, significative differences in the bands appearing between 550 to 1500 cm^{-1} (Figure S2b) were spotted indicating a structural change between the CLIP precursor and the as-synthesized NaP1 zeolites, consistent with previous findings [20].

EDS data (Figure S3) show the presence of Si, Al, O, and Na atoms, comprising the NaP1-type zeolite, showing that Na^+ ions are the main counter-balancing cations in the zeolite structure [31], along with traces of K^+ and Ca^{2+} detected in the point analysis. This result is similar to that of NaP1 zeolites from fly ash, where extra-framework cations such as K^+, Ca^{2+}, Mg^{2+}, and Fe^{2+} have been detected [32, 33]. Furthermore, an average Si/Al molar ratio of 1.7 is obtained, which is in the range of 1.1-2.5, is typical for NaP-type zeolites [28, 34]. It has been reported that such variations in Si/Al ratio depend on zeolite synthesis conditions [25]. The high-resolution XPS spectrum (Figure S4) shows the presence of O1s (531.58 eV), Si2p (102.48 eV), Al2p (74.38 eV), and Na1s (1072.28 eV) photoelectron lines, where the signal in the O1s region displayed a band at 531.58 eV ascribed to the oxygen of the X–O (X

= Si, Al, Na) bonds in zeolites [35], and a small peak at 537.28 eV corresponding to the sodium Auger (Na KLL Auger) overlapping with the O1s region [36], generated by the sodium located inside the zeolite scaffold. In addition, a Si/Al ratio of 1.58, which is comparable to the EDS results, was determined, confirming the presence of K^+ and Ca^{2+} traces.

In addition, TGA analysis was conducted to investigate the water content of the as-synthesized NaP1 zeolite with 1 M NaOH for 24 h at 90 °C. TGA (Figure S5) reveals a total weight loss of about 13.5 wt% by 500 °C and this happens in two steps. The first step, in the temperature range between 62.5 and 250 °C, the mass loss can be ascribed to the removal of water molecules inside the zeolite micropores, where the maximal weight loss for this area is located at around 100 °C. The second weight loss region occurs between 250 up to 500 °C, and has been previously assigned to the decomposition and removal of hydroxyl groups in the as-synthesized NaP1 sample with maximum loss at around 325 °C [28, 37]. The thermal stability of the as-synthesized NaP1 zeolite with 1 M NaOH for 24 h at 90 °C was also analyzed, proving that a thermal treatment at 450 °C did not affect the well-defined zeolite structure [7], as confirmed by the X-ray diffraction patterns (Figure S6). This preservation of the structure was consistent when compared to the non-calcined sample and with previous reports [7].

In contrast, in the second test, the alkalinity of the NaOH solution was increased to 2 M for 24 h and to 90 °C for HT. Nevertheless, the XRD results (Figure S7) show an amorphous phase with some peaks belonging to the NaP1 zeolite (JCPDS No. 71-0962) [8, 22, 25]. The SEM micrographs (Supplementary Figure S8) show crystals with undefined morphologies and the appearance of irregular P-type zeolite-phase crystals. These results suggest that an increase in alkalinity strongly influences the production of NaP1-type zeolites. As suggested in the literature [31, 38], alkalinity plays an important role, as it significantly affects the nucleation and crystalline growth of zeolites. Therefore, high-alkalinity conditions can suddenly transform the synthesized NaP zeolite because of an increase in the crystallization rate through crystal growth and nucleation, which is a consequence of the increase in the concentrations of aluminates, silicates, and aluminosilicates [12], suggesting that mild synthesis conditions of 1 M for 24 h at 90 °C are suitable for the formation of a pure NaP1 phase.

3.3 Effect of temperature on the crystallization of as-synthesized NaP1 zeolites

The crystallization temperature was increased to 105 °C while maintaining the 1 M and 24 h synthesis conditions. The resulting XRD pattern (Figure S9) shows well-defined profiles owing to the formation of NaP1-type zeolites [22]. This observation suggests that the increase in temperature did not contribute to the formation of a new zeolite phase, and the crystallinity of the NaP zeolite was not affected. Nevertheless, SEM micrographs (Figures 4a and b) reveal changes in the crystal morphology compared to those of previous NaP1 zeolites obtained at 1 M for 24 h at 90 °C (Figure 3b), displaying a larger crystal size (~10 µm, Supplementary Figure S10) and a cheese ball-like shape characteristic of NaP1 zeolite, similar to those reported elsewhere [3, 19, 21, 39]. Nonetheless, the presence of impurity crystal phases such as LTA- and FAU-like crystals are detected (Figures 4c and d). It must be noted that at 105 °C, a zeolite in the process of recrystallization is obtained, giving rise to macro-cracks (Figure 4b), which divided the zeolite into smaller sections. This can be attributed to a possible phase transformation of the zeolite, which involves a decrease in the volume of the crystalline unit cell. As a result, it is expected that stress will develop, leading to cracks in the zeolite layer owing to a structural transition [40]. Hong S. *et al.* [21] reported a similar phenomenon during the synthesis of NaP zeolite from Korean natural CLIP using a "top-down approach".

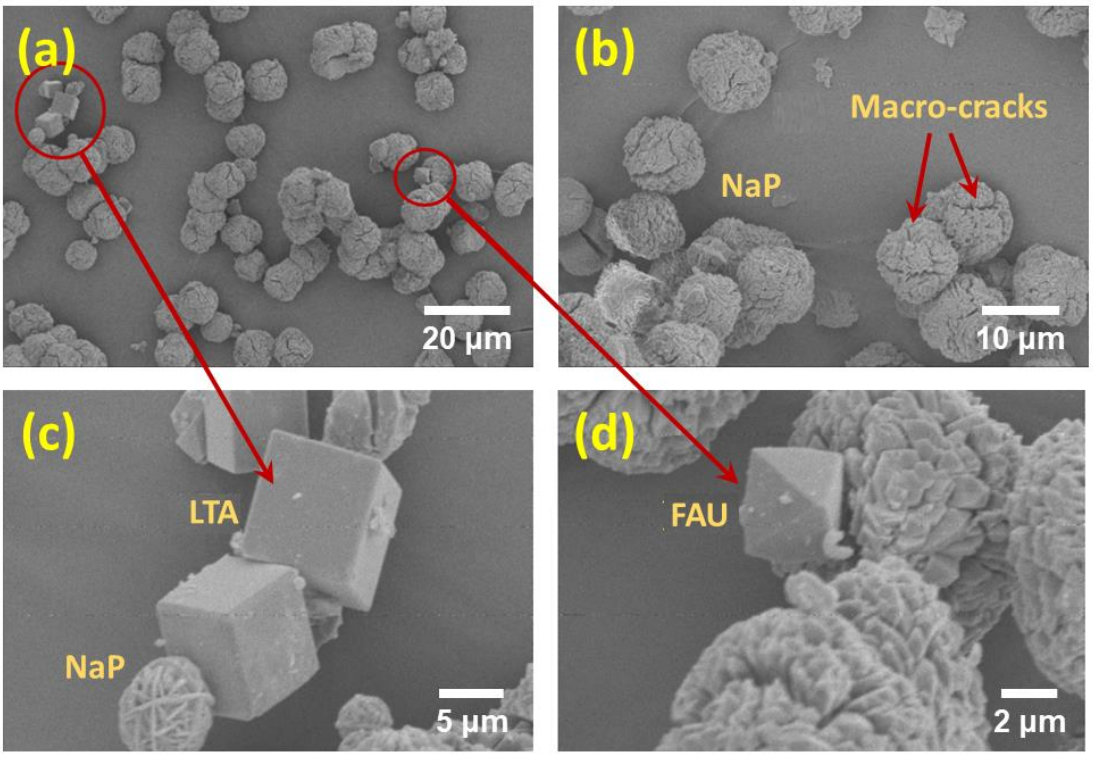

Figure 4. (a-d) SEM micrographs of zeolite crystals obtained from synthesis with 1 M NaOH for 24 h at 105 °C.

The structural transformation of zeolites with increasing temperature and/or synthesis time can be explained according to the Ostwald law of successive transformations (or rule of stages), which establishes that the first type of zeolite to be formed tends to be the least stable (or metastable phase) and is preferentially replaced by more thermodynamically stable forms [41]. However, the transformation of NaP1 zeolite (16.4 T/1000 $Å^3$) to LTA (14.2 T/1000 $Å^3$) or FAU (13.3 T/1000 $Å^3$) zeolites contradicts the trend predicted by Ostwald's rule of stages, since this sequence involves a transformation from a larger density structure to one that is less dense, and thus less thermodynamically stable [6]. In addition, it appears counter-intuitive that no intermediary FAU and LTA crystals are observed in the synthesis with 1 M NaOH performed at 90 °C, but were observed in the product synthesized at 105 °C. This irregularity could have been produced by the dissolution of some CLIP crystals, forming TO_4 units that rearranged to directly form the FAU or LTA phase [20], thereby explaining the presence of a few remaining FAU and LTA crystals. Interestingly, the SEM micrographs also show the presence of wool ball-shaped NaP zeolites next to LTA crystals, as shown in Figure 4c. Huo *et al.* [25] reported the synthesis of NaP zeolites by employing sodium silicate and sodium aluminate and adjusting certain reaction parameters to obtain different morphologies, such as cactus-, diamond-, and wool ball-shapes, attributing the morphology type variation to

the Si/Al ratio, as a determining factor to obtain a certain shape. Thus, the formation of impurity phases (LTA-, FAU-like crystals, and wool-ball-shaped NaP zeolites) could be related to specific Si- or Al-rich regions during the crystallization process.

3.4 Obtaining as-synthesized NaP2 zeolites by varying temperature and crystallization time

Currently, there is a great demand for porous materials capable of separating small gases, such as CH_4, CO_2, N_2, and H_2. Small-pore zeolites are promising candidates because of their high sorption capacity and selectivity. In this regard, NaP zeolites have proven to be good candidates for CO_2 adsorption because they exhibit exceptional framework flexibility, generating two polymorphs, NaP1 and NaP2 [42]. In addition, it has been reported that the NaP2 zeolite has a higher adsorption equilibrium constant for H_2 [7]. To obtain new phases of NaP zeolite, in a subsequent test using a NaOH concentration of 2 M, the crystallization temperature and crystallization time were increased to 110 °C and 39 h, respectively. By analyzing the XRD pattern of the new product, several peaks distinct from the characteristic peaks of the NaP1-type zeolite were observed, as shown in Figure 5. Oleksiak *et al.* [7] explained that despite NaP1 and NaP2 polymorphs present similar crystalline morphology, it is possible to differentiate the crystalline structure of each of them through their XRD patterns. They also mentioned that it is uncommon to find an experimental XRD pattern for the NaP2 zeolite, even in the IZA structure database [22]. Nevertheless, the NaP2 zeolite pattern was simulated using the JCPDS 01-80-0700 reference file, which is based on the crystallographic data from Hansen *et al.* [43], and compared with the XRD pattern of the as-synthesized material. As indicated by the XRD pattern (Figure 5), the main phase of the sample corresponds to the NaP2-type zeolite, with some split peaks associated with two rotating types of SBUs planes or 4MR in the GIS-type structure [7, 39], which have not been completely formed, as observed in the shaded regions of the XRD spectrum, which could be indicative of a zeolite still in the crystallization process. Nonetheless, the FTIR spectra of NP2 zeolites (Figure S11) display similar bands to those corresponding to the as-synthesized NaP1 zeolite obtained from the synthesis with 1 M NaOH for 24 h at 90 °C (Figure S2).

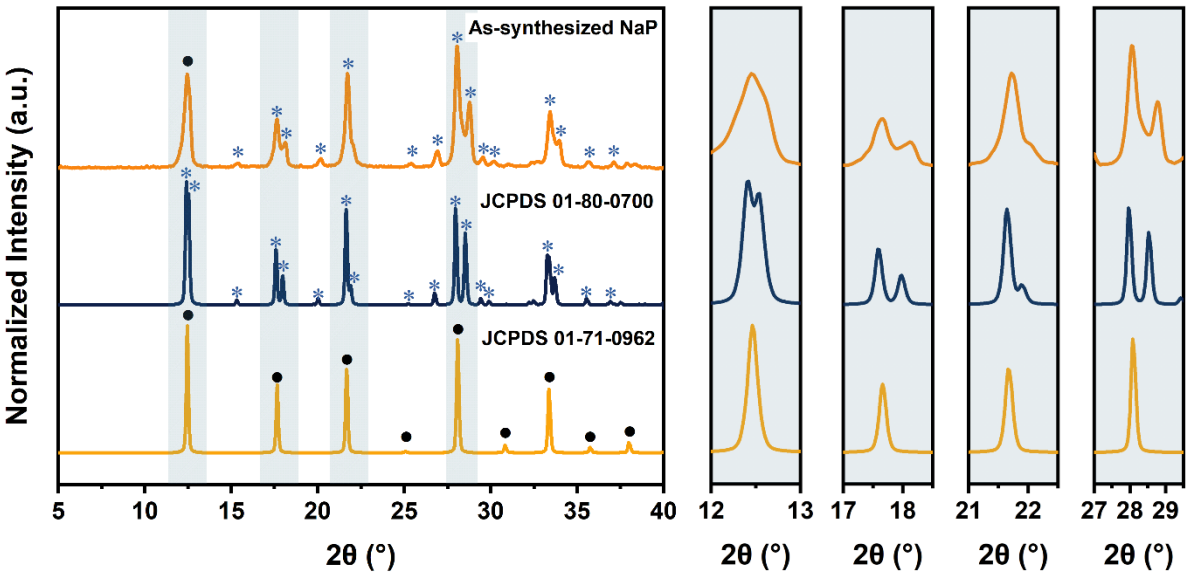

Figure 5. XRD pattern of the as-synthesized NaP zeolite obtained from the synthesis with 2 M NaOH for 39 h at 110 °C confirmed that the main phase was NaP2 zeolite. The XRD pattern of NaP2 (JCPDS 01-080-0700) was simulated following the procedure described by Oleksiak *et al*. [7] using the crystallographic data from Hansen *et al*. [43], whereas the pattern of NaP1 (JCPDS 01-71-0962) was obtained from the IZA structure database [22].

Likewise, SEM micrographs with different magnifications of the as-synthesized NaP2 are depicted in Figures 6a-c. Under these hydrothermal conditions, it was also possible to observe the formation of macro-cracks in zeolites with a cheese ball-shape [21] (Figure 6a), resulting in smaller zeolites with an amorphous diamond-like morphology and some with trisecting cracks (Figures 6b and c), with an average particle size of 4.2 µm (Figure 6d). Although the sample has various shapes and morphologies, the XRD results (Figure 5) mainly indicated the NaP2 phase. Moreover, these morphologies are similar to those of the NaP2-type zeolites reported elsewhere [5, 39, 44]. The formation of cracks in this sample suggests an interzeolitic transformation of zeolite with a smaller crystalline unit cell volume [40]. It has been reported that the framework density of NaP2 zeolite is higher than that of NaP1 zeolite owing to its smaller pore size [7, 39]. Therefore, these findings fully agree with Ostwald's rule of stages for the conversion of a metastable zeolite into a denser and thermodynamically stable crystalline structure [6, 41]. Recently, Boudia *et al.* [45] found similar results in obtaining an interzeolitic transition from NaP1 to NaP2 by performing pretreatment, alkaline fusion, and magnetic stirring in an alkaline solution to extract Si and Al from clay fractions > 2 µm, where the supernatant was subjected to hydrothermal activation for six days to obtain NaP2 with a Si/Al ratio of approximately 1.81. This is in good

agreement with our results, where an average Si/Al ratio of 1.88 is obtained (Supplementary Figure S11), and similar to that reported for NaP2-type zeolites obtained by conventional hydrothermal synthesis [39].

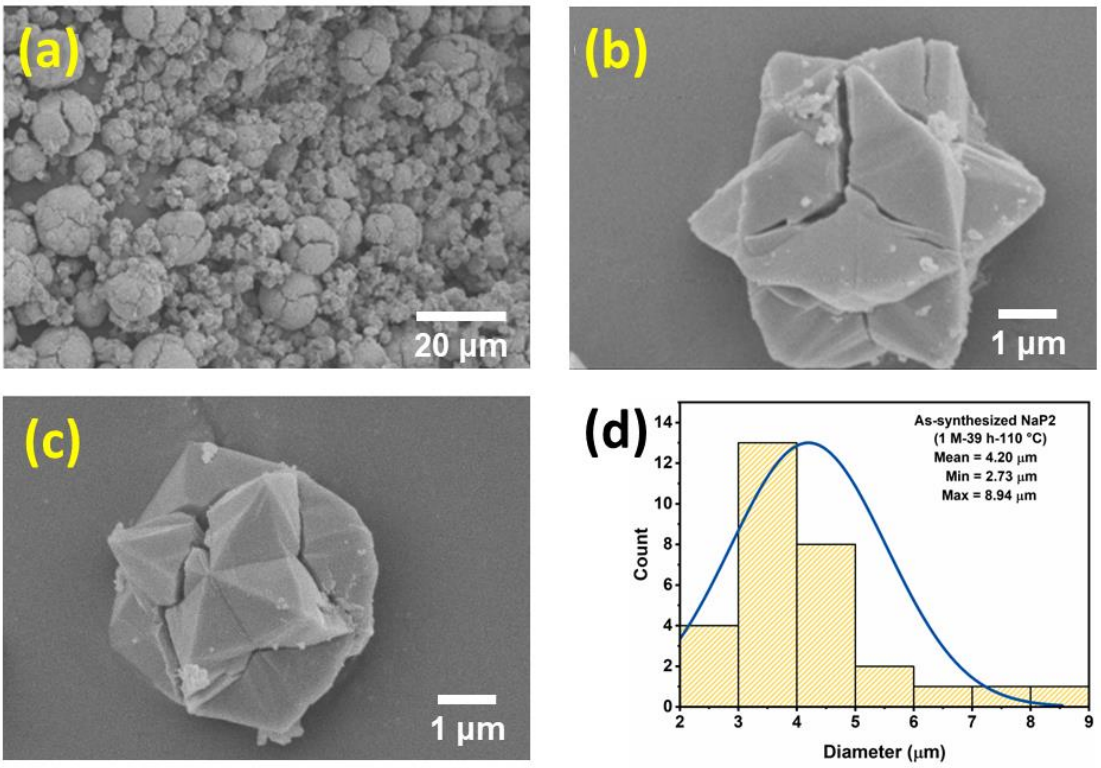

Figure 6. (a-c) SEM micrographs and particle size distribution analyzed by ImageJ (calculated from 30 to 50 particles) of the zeolite product obtained from synthesis with 2 M NaOH for 39 h at 110 °C under different magnifications.

Previous studies have reported the production of NaP2 from NaY gel [39, 44]. For instance, Tayraukham *et al.* [39] obtained a pure phase NaP2 zeolite from NaY gel as a precursor by a conventional hydrothermal method at 150 °C for 24 h and from double crystallization by a microwave-assisted hydrothermal method in three steps: (1) crystallization at 90 °C for 1 h and rapid cooling to room temperature in the microwave chamber; (2) aging at room temperature for 23 h; and (3) crystallization at 150 °C for 1 h. However, commercial chemical reagents were used as Si and Al sources for gel preparation. In the present report, a similar NaP2 was obtained, but using an abundant low-cost natural precursor and a simpler method with mild synthesis conditions (2 M NaOH for 39 h at 110 °C), demonstrating the feasibility of our proposal.

4. CONCLUSIONS

The synthesis of two small-pore NaP-type zeolites with a flexible framework using natural CLIP as a source of Si and Al via a hydrothermal process is presented. We show that the alkaline dissolution of CLIP leads to the direct crystallization of two NaP-type zeolite isomorphs (NaP1 and NaP2) and that the synthesis conditions of 1 M for 24 h at 90 °C led to the formation of a single-phase NaP1 zeolite with high purity. Similarly, we demonstrated that by varying the synthesis parameters such as the crystallization temperature (1 M for 24 h at 105 °C), it is possible to obtain different morphologies of the NaP1-type zeolite with a larger crystal size (~10 μm). Moreover, a direct phase transformation from NaP1 to NaP2 zeolite, which has a smaller pore size, was also observed with increasing crystallization temperature (110 °C) and crystallization time (39 h), making it attractive for the separation of small gases. From an economic and environmental point of view, these results demonstrate that natural CLIP used as a source of Si and Al is a cost-effective, readily available, and abundant mineral, making it an excellent low-cost resource for the manufacture of high-value-added zeolites. This provides a platform for extending the use of these starting materials to other types of synthesis methods such as dry solid fused alkali reagents to obtain different types of industrially appealing zeolites such as NaP, FAU, LTA, and SOD, and focused on specific applications such as the separation of small gases (CO_2 and H_2).

ASSOCIATED CONTENT

Supplementary Information. Zeolite characterization, SEM-EDS analysis, XPS, and XRD results. This material is available free of charge on the Internet.

AUTHOR INFORMATION

Corresponding Authors
*Email: rrbon@cinvestav.mx, ecoutino@vito.be

Author Contributions

J.A.M.-T.: Methodology, Formal Analysis, Validation, Writing—original draft, Writing—review & editing. **F.E.-A.**: Methodology, Validation, Investigation, Writing—original draft, Writing—review & editing. **R.R.-B.**: Conceptualization, Methodology, Investigation, Writing—original draft, Validation, Writing—review & editing. **E.C.-G.**: Conceptualization, Methodology, Investigation, Writing—original draft, Validation, Writing—review & editing,

Funding acquisition. All authors have read and agreed to the published version of the manuscript.

Notes

The authors declare no competing financial interests.

ACKNOWLEDGMENT

E.C.-G gratefully acknowledges the financial support from CONACYT through the CB-A1-S-44458 and 2096029-FORDECYT-PRONACES grants. J.A.M.-T acknowledges the support from a CONACYT PhD scholarship (743221). We also acknowledge the technical support provided by the M.C. Christian Albor Cortes from Centro de Investigaciones en Óptica, A.C. for providing SEM-EDS analyses of the samples.

REFERENCES

1. Sánchez-Hernández R, López-Delgado A, Padilla I, et al (2016) One-step synthesis of NaP1, SOD and ANA from a hazardous aluminum solid waste. Microporous Mesoporous Mater 226:267–277. https://doi.org/10.1016/j.micromeso.2016.01.037
2. Dusselier M, Davis ME (2018) Small-Pore Zeolites: Synthesis and Catalysis. Chem Rev 118:5265–5329. https://doi.org/10.1021/acs.chemrev.7b00738
3. Sharma P, Song JS, Han MH, Cho CH (2016) GIS-NaP1 zeolite microspheres as potential water adsorption material: Influence of initial silica concentration on adsorptive and physical/topological properties. Sci Rep 6:1–26. https://doi.org/10.1038/srep22734
4. McCusker LB, Olson DH, Baerlocher C (2007) GIS—I41/amd. In: Atlas of Zeolite Framework Types, 6th ed. Elsevier Science B.V.: Amsterdam, The Netherlands, pp 146–147
5. Albert BR, Cheetham AK, Stuart JA, Adams CJ (1998) Investigations on P zeolites: Synthesis, characterisation, and structure of highly crystalline low-silica NaP. Microporous Mesoporous Mater 21:133–142. https://doi.org/10.1016/S1387-1811(97)00059-0
6. Maldonado M, Oleksiak MD, Chinta S, Rimer JD (2013) Controlling crystal polymorphism in organic-free synthesis of na-zeolites. J Am Chem Soc 135:2641–2652. https://doi.org/10.1021/ja3105939
7. Oleksiak MD, Ghorbanpour A, Conato MT, et al (2016) Synthesis Strategies for Ultrastable Zeolite GIS Polymorphs as Sorbents for Selective Separations. Chem - A Eur J 22:16078–16088. https://doi.org/10.1002/chem.201602653
8. Baerlocher C, Meier WM (1972) The crystal structure of synthetic zeolite na-p 1, an isotype of gismondine. Zeitschrift fur Krist - New Cryst Struct 135:339–354. https://doi.org/10.1524/zkri.1972.135.5-6.339
9. Deneyer A, Ke Q, Devos J, Dusselier M (2020) Zeolite Synthesis under Nonconventional Conditions: Reagents, Reactors, and Modi Operandi. Chem Mater 32:4884–4919. https://doi.org/10.1021/acs.chemmater.9b04741
10. Khaleque A, Alam MM, Hoque M, et al (2020) Zeolite synthesis from low-cost materials and environmental applications: A review. Environ Adv 2:.

https://doi.org/10.1016/j.envadv.2020.100019
11. Azizi D, Ibsaine F, Dionne J, et al (2021) Microporous and macroporous materials state-of-the-art of the technologies in zeolitization of aluminosilicate bearing residues from mining and metallurgical industries: A comprehensive review. Microporous Mesoporous Mater 318:. https://doi.org/10.1016/j.micromeso.2021.111029
12. Pangan N, Gallardo S, Gaspillo PA, et al (2021) Hydrothermal synthesis and characterization of zeolite a from corn (Zea mays) stover ash. Materials (Basel) 14:. https://doi.org/10.3390/ma14174915
13. Wang Y, Lin F (2009) Synthesis of high capacity cation exchangers from a low-grade Chinese natural zeolite. J Hazard Mater 166:1014–1019. https://doi.org/10.1016/j.jhazmat.2008.12.001
14. Behin J, Kazemian H, Rohani S (2016) Sonochemical synthesis of zeolite NaP from clinoptilolite. Ultrason Sonochem 28:400–408. https://doi.org/10.1016/j.ultsonch.2015.08.021
15. Sánchez-Ruíz A, Robles-Gutiérrez I, Espejel-Ayala F (2018) Preparation of zeolitic material using natural clinoptilolite for CO_2 capture. Rev Mex Ing Quim 17:573–585. https://doi.org/10.24275/uam/izt/dcbi/revmexingquim/2018v17n2/Sanchez
16. de las Pozas C, Díaz Quintanilla D, Pérez-Pariente J, et al (1989) Hydrothermal transformation of natural clinoptilolite to zeolites Y and P1: Influence of the Na, K content. Zeolites 9:33–39. https://doi.org/10.1016/0144-2449(89)90006-7
17. Kang SJ, Egashira K (1997) Modification of different grades of Korean natural zeolites for increasing cation exchange capacity. Appl Clay Sci 12:131–144. https://doi.org/10.1016/S0169-1317(97)00002-1
18. Kang SJ, Egashira K, Yoshida A (1998) Transformation of a low-grade Korean natural zeolite to high cation exchanger by hydrothermal reaction with or without fusion with sodium hydroxide. Appl Clay Sci 13:117–135. https://doi.org/10.1016/S0169-1317(98)00019-2
19. De Fazio A, Brotzu P, Ghiara MR, et al (2008) Hydrothermal treatment at low temperature of Sardinian clinoptilolite-bearing ignimbrites for increasing cation exchange capacity. Period di Mineral 77:79–91. https://doi.org/10.2451/2008PM0006
20. de Lima RCF, da Silva Oliveira D, Pergher SBC (2021) Interzeolitic transformation of clinoptilolite into GIS and LTA zeolite. Minerals 11:. https://doi.org/10.3390/min11121313
21. Hong S, Um W (2021) Top-down synthesis of NaP zeolite from natural zeolite for the higher removal efficiency of Cs, Sr, and Ni. Minerals 11:1–15. https://doi.org/10.3390/min11030252
22. IZA Copyright © 2017 Structure Commission of the International Zeolite Association Database of Zeolite Structures. http://www.iza-structure.org/databases/. Accessed 20 Dec 2022
23. Dimowa L, Tzvetanova Y (2021) Powder xrd study of changes of cd2+ modified clinoptilolite at different stages of the ion exchange process. Minerals 11:. https://doi.org/10.3390/min11101130
24. Abdullahi T, Harun Z, Othman MHD (2017) A review on sustainable synthesis of zeolite from kaolinite resources via hydrothermal process. Adv Powder Technol 28:1827–1840. https://doi.org/10.1016/j.apt.2017.04.028
25. Huo Z, Xu X, Lü Z, et al (2012) Synthesis of zeolite NaP with controllable morphologies. Microporous Mesoporous Mater 158:137–140. https://doi.org/10.1016/j.micromeso.2012.03.026
26. Zubowa HL, Kosslick H, Müller D, et al (2008) Crystallization of phase-pure zeolite NaP from MCM-22-type gel compositions under microwave radiation. Microporous

Mesoporous Mater 109:542–548. https://doi.org/10.1016/j.micromeso.2007.06.002
27. Hildebrando EA, Andrade CGB, Da Rocha Junior CAF, et al (2014) Synthesis and characterization of zeolite NaP using kaolin waste as a source of silicon and aluminum. Mater Res 17:174–179. https://doi.org/10.1590/S1516-14392014005000035
28. Ali IO, El-Sheikh SM, Salama TM, et al (2015) Controllable synthesis of NaP zeolite and its application in calcium adsorption. Sci China Mater 58:621–633. https://doi.org/10.1007/s40843-015-0075-9
29. Shameli K, Ahmad M Bin, Zargar M, et al (2011) Fabrication of silver nanoparticles doped in the zeolite framework and antibacterial activity. Int J Nanomedicine 6:331–341. https://doi.org/10.2147/ijn.s16964
30. Youssef HF, Hegazy WH, Abo-Almaged HH, El-Bassyouni GT (2015) Novel synthesis method of micronized Ti-Zeolite Na-A and cytotoxic activity of its silver exchanged form. Bioinorg Chem Appl 2015:. https://doi.org/10.1155/2015/428121
31. Sánchez-Hernández R, Padilla I, López-Andrés S, López-Delgado A (2017) Eco-friendly bench-scale zeolitization of an Al-containing waste into gismondine-type zeolite under effluent recycling. J Clean Prod 161:792–802. https://doi.org/10.1016/j.jclepro.2017.05.201
32. Franus W, Wdowin M, Franus M (2014) Synthesis and characterization of zeolites prepared from industrial fly ash. Environ Monit Assess 186:5721–5729. https://doi.org/10.1007/s10661-014-3815-5
33. Cardoso AM, Paprocki A, Ferret LS, et al (2015) Synthesis of zeolite Na-P1 under mild conditions using Brazilian coal fly ash and its application in wastewater treatment. Fuel 139:59–67. https://doi.org/10.1016/j.fuel.2014.08.016
34. Bohra S, Kundu D, Naskar MK (2013) Synthesis of cashew nut-like zeolite NaP powders using agro-waste material as silica source. Mater Lett 106:182–185. https://doi.org/10.1016/j.matlet.2013.04.080
35. Barr TL (1990) The nature of the relative bonding chemistry in zeolites: An XPS study. Zeolites 10:760–765. https://doi.org/10.1016/0144-2449(90)90058-Y
36. Zhan X, Shirpour M (2017) Evolution of solid/aqueous interface in aqueous sodium-ion batteries. Chem Commun 53:204–207. https://doi.org/10.1039/C6CC08901A
37. Huo Z, Xu X, Lv Z, et al (2013) Thermal study of NaP zeolite with different morphologies. J Therm Anal Calorim 111:365–369. https://doi.org/10.1007/s10973-012-2301-y
38. Meng X, Guo X, Zhong Y, et al (2019) Synthesis of a high-quality NaP zeolite from epidesmine by a hydrothermal method. Bull Mater Sci 42:1–8. https://doi.org/10.1007/s12034-019-1918-x
39. Tayraukham P, Jantarit N, Osakoo N, Wittayakun J (2020) Synthesis of pure phase NaP2 zeolite from the gel of NaY by conventional and microwave-assisted hydrothermal methods. Crystals 10:1–11. https://doi.org/10.3390/cryst10100951
40. Dong J, Lin YS (1998) In situ synthesis of P-type zeolite membranes on porous α-alumina supports. Ind Eng Chem Res 37:2404–2409. https://doi.org/10.1021/ie970851o
41. Katović A, Subotić B, Šmit I, Despotović LA (1989) Crystallization of tetragonal (B8) and cubic (B1) modifications of zeolite NaP from freshly prepared gel. Part 1. Mechanism of the crystallization. Zeolites 9:45–53. https://doi.org/10.1016/0144-2449(89)90008-0
42. Choi HJ, Min JG, Ahn SH, et al (2020) Framework flexibility-driven CO2 adsorption on a zeolite. Mater Horizons 7:1528–1532. https://doi.org/10.1039/d0mh00307g
43. Hansen S, Håkansson U, Fälth L (1990) Structure of synthetic zeolite Na-P2. Acta Crystallogr Sect C Cryst Struct Commun 46:1361–1362.

https://doi.org/10.1107/s010827018901262x
44. Le T, Wang Q, Pan B, et al (2019) Process regulation of microwave intensified synthesis of Y-type zeolite. Microporous Mesoporous Mater 284:476–485. https://doi.org/10.1016/j.micromeso.2019.04.029
45. Boudia RA, Bendeddouche CK, Mazari MM, et al (2023) Zeolite GIS Polymorphs Derived from Clay Fraction > 2 µm: The Ability of Clay Fraction > 2 µm for Crystallization of High-Purity Na-P1 Zeolite. Silicon. https://doi.org/10.1007/s12633-023-02335-4